Electronic Supplementary Information

Tailoring surface plasmons of high-density gold nanostar assemblies on metal films for surface-enhanced Raman spectroscopy

Jiwon Lee[†,§], *Bo Hua*[‡,§], *Seungyoung Park*[†], *Minjeong Ha*[†], *Youngsu Lee*[†], *Zhiyong Fan*[*,‡], *and Hyunhyub Ko*[*,†]

[†]School of Energy and Chemical Engineering, Ulsan National Institute Science and Technology (UNIST), Ulsan, Republic of Korea.

[‡]Department of Electronic & Computer Engineering, Hong Kong University of Science & Technology (HKUST), Hong Kong SAR, China.

[§]These authors contributed equally.

Corresponding Author

[*]hyunhko@unist.ac.kr, eezfan@ust.hk

SERS intensities as a function of GNS surface density

Figure S6 shows the variation in the SERS intensity as a function of the GNS surface density on Ag and glass substrates. For a GNS array on the Ag film, the SERS intensities increased as the GNS surface density increased for surface densities below ~43 GNSs/μm^2, and slowly decreased with a further increase in the GNS surface density (Figure S6a). For GNS assemblies on glass surfaces, the SERS intensities increased exponentially as the surface density increased (Figure S6b). These two different behaviors of SERS intensities with an increase in the GNS surface density can be explained by the interplay between the interparticle and the particle–film plasmon couplings on Ag and glass surfaces. As the surface density of the GNS assemblies on Ag films increased, the SERS intensity increased as well due to the increased number of hot spots at the GNS–Ag gaps. However, as the surface density continued to increase, it reached a certain point where the strong interparticle couplings interfered with the particle–film couplings, resulting in a decrease in the SERS intensity. In contrast, because the EF increased monotonically on the glass surface as the interparticle distance decreased, an increase in the GNS surface density on the glass surface led to a monotonic increase in the Raman intensity, as shown in Figure S6b.

The FDTD results of the field enhancement from interparticle and particle–film couplings were closely related to the overall average SERS enhancements. Because the SERS intensity is proportional to the fourth power of the local E-field enhancement, the SERS enhancement factor (EF) can be approximated as $EF = (|E/E_0|^4)$, where E and E_0 represent the local and incident E-fields, respectively.[1] Additionally, the SERS intensity is proportional to the number of SERS hot spots under the laser exposure area. Therefore, to estimate the

ensemble-averaged EF from GNS assemblies, we normalized the EF with respect to the density of hot spots, which is proportional to GNS surface density on a substrate. To achieve a more quantitative estimation, we assumed that each GNS in the hexagonal array contributed four hot spots from GNS–film coupling, and one hot spot from GNS–GNS coupling, even though other configurations were possible; however, this should not change the overall trend. Therefore, the GNS density-normalized EF (EF_N) can be approximated as $EF_N = (4|E/E_0|^4_{GNS\text{-}film} + (|E/E_0|^4_{GNS\text{-}GNS}) \times$ (GNS surface density). Figure S6c shows the normalized EF as a function of GNS density for GNS assemblies on Ag films. EF_N increased as the surface density increased up to a density of ~68 GNSs/μm^2, and decreased as the surface density was increased further. This trend qualitatively agreed well with the experimental SERS intensity as a function of surface density (Figure S6a), where the SERS intensities increased at first and then slowly decreased for surface densities over ~43 GNSs/μm^2. For the GNSs on the glass substrate, the EF_N exponentially increased with an increase in the surface density (Figure S6d), which is also in good agreement with the experimental results shown in Figure S6b.

SERS comparision of gold nanostars vs. nanospheres

GNSs, with their sharp tips, are expected to have strong interparticle plasmon couplings, especially when they are arranged into bowtie antenna pairs. It is well known that the bowtie antenna pairs, a triangular metallic nanostructure with a nanometer-scale gap between two facing tips, have strong E-fields enhancements in the gap regions due to the so-called "lightning rod effect" at the sharp end of the tip, in addition to the plasmon couplings commonly observed in dipole antenna.[2] Additionally, the sharp tips of GNSs on gold films

have demonstrated strong E-field enhancements, resulting in SERS enhancement factors of up to ~10^{10}.[3]

The sharp tips of GNSs can have a significant effect on the SERS enhancements of high-density nanostars on metal films. The strong E-fields confined at the ends of the sharp tips due to the lightning rod effect are likely to further enhance plasmon couplings between nanostars and also between nanostars and films. However, as compared with GNSs, Au nanospheres without any sharp tips will provide weaker field enhancements at the interparticle and particle–film gap regions, wherein SERS intensities are expected to be lower than the system of GNSs on metal films. Figure S8a shows the SERS spectra of benzenethiol (100 mM) adsorbed on GNSs or nanospheres assembled on Ag films. As expected, SERS spectra of benzenethiol molecules adsorbed on GNSs/Ag films showed a much higher SERS intensity (~52× higher) than those on Au nanospheres/Ag films for the C–C symmetric stretching and C–S stretching at 1072 cm^{-1}. Simulation results also revealed that the E-field intensity in particle–film gap of the GNSs was ~18× stronger than that for Au nanospheres having a similar particle size (Figure S8b,c).

The effects of gap distance between GNS and substrates

The gap distance between the GNS and the Ag film was controlled by using layer-by-layer (LbL) polymer multilayers, where positively-charged poly(diallyldimethylammonium) (PDDA) and negatively-charged poly(sodium 4-styrenesulfonate) (PSS) polymers are alternatively deposited on the Ag substrate. In a typical process, the substrate was coated with polymers via spin-coating (4000rpm, 60s) the polymer solution (0.2 wt% in water) and rinsing with ultra-pure water twice. The above process was repeated to fabricate polymer

layers of PDDA, (PDDA/PSS)PDDA, $(PDDA/PSS)_2PDDA$, and $(PDDA/PSS)_4PDDA$, resulting in different gap distances. Ellipsometry measurents confirmed that the thickness of the polymer layers was 0.8, 1.7, 2.5, and 4.4 nm for the PDDA, (PDDA/PSS)PDDA, $(PDDA/PSS)_2PDDA$, and $(PDDA/PSS)_4PDDA$ layers (Figure S12a). The different gap distances significantly affect the GNS-Ag film couplings. The SERS intensity of the GNS-Ag film system continuously decreases when the gap distance increases from 0.8 to 4.4 nm, demonstrating the dominant role of GNS-Ag film couplings in the SERS enhancements. The change of GNS-Ag film plasmon couplings with the variation of gap distances is also verified by the optical reflectance measurements. Figure S12c indicates that the reflectance deep continuously shifts from 539 to 581 nm when the gap distance changes from 0.8 to 4.4 nm.

SERS Enhancement factor calculations

For the calculation of experimental SERS enhancement factors, we used a standard equation[4]

$$\text{SERS EF}=\frac{I_{SERS}/N_{SERS}}{I_{ref}/N_{ref}}$$

where I_{SERS} and I_{ref} are the intensities of Raman band on SERS and reference substrates, N_{SERS} and N_{ref} are the number of molecules probed on SERS and reference substrates. I_{SERS} and I_{ref} are measured using the Raman band of the 1072 cm^{-1} for the BT molecules. N_{SERS} is calculated based on the assumption of monolayer packing (packing density of 6.8×10^{14} molecules/cm^2)[5] of BT molecules on the GNS surface and the metal (Ag, Au) substrates. N_{ref} is calculated based on the estimation of active volume with the information of the laser spot size[6] of ~2.5 μm and the confocal depth of focus[7] of 6.8 μm for the pure BT solution (Mw:110.19 g/mol, density:1.073 g/ml).

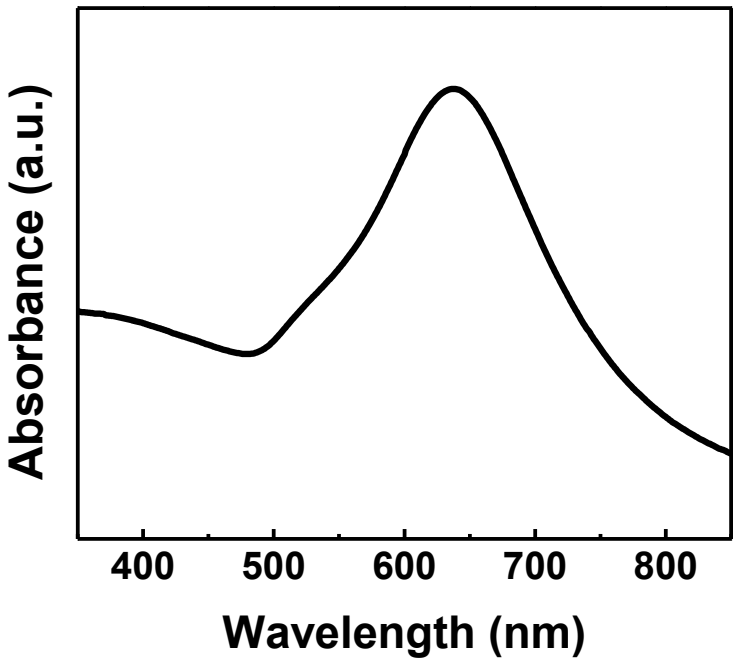

Figure S1. Ultraviolet–visible (UV–Vis) spectrum of the GNS solution showing a localized surface plasmon resonance (LSPR) peak at ~640 nm.

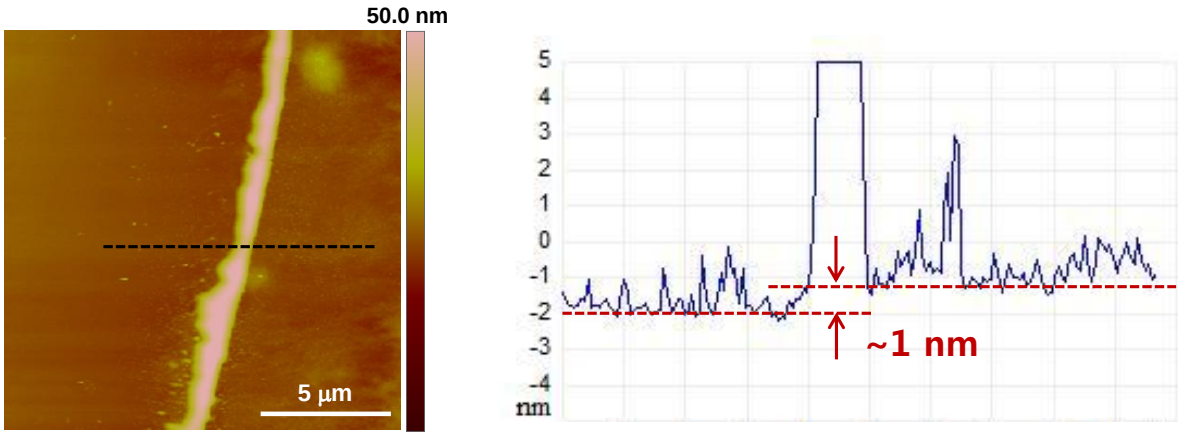

Figure S2. AFM image of 0.2 % PDDA coated on Si substrate. The cross-section analysis showed a representative area with PDDA thickness in the range ~1 nm.

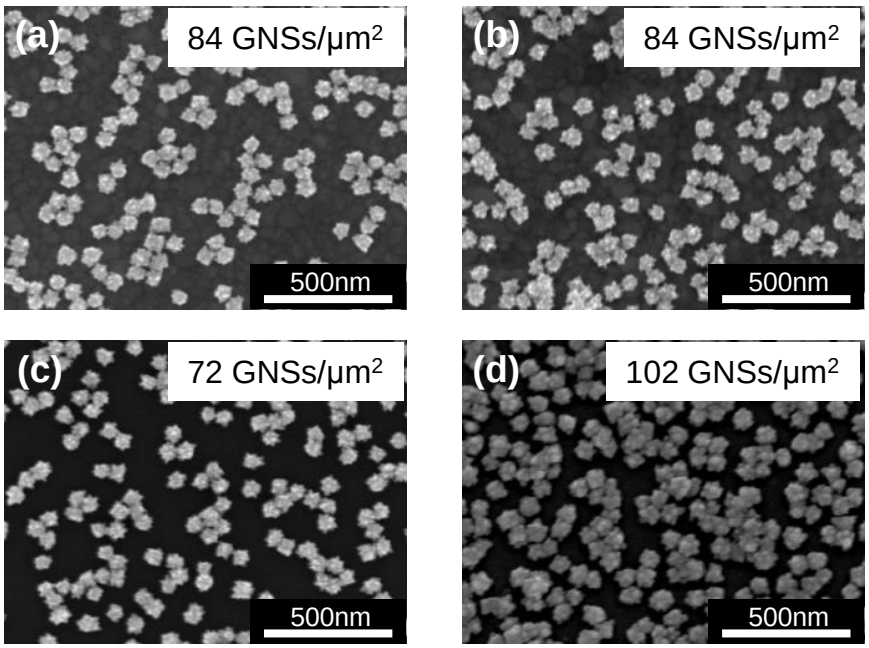

Figure S3. FE-SEM images of GNSs on different substrates;Ag film (a), Au film (b), Silicon substrate (c), and cover slip glass (d). GNS surface densities are marked on the figures.

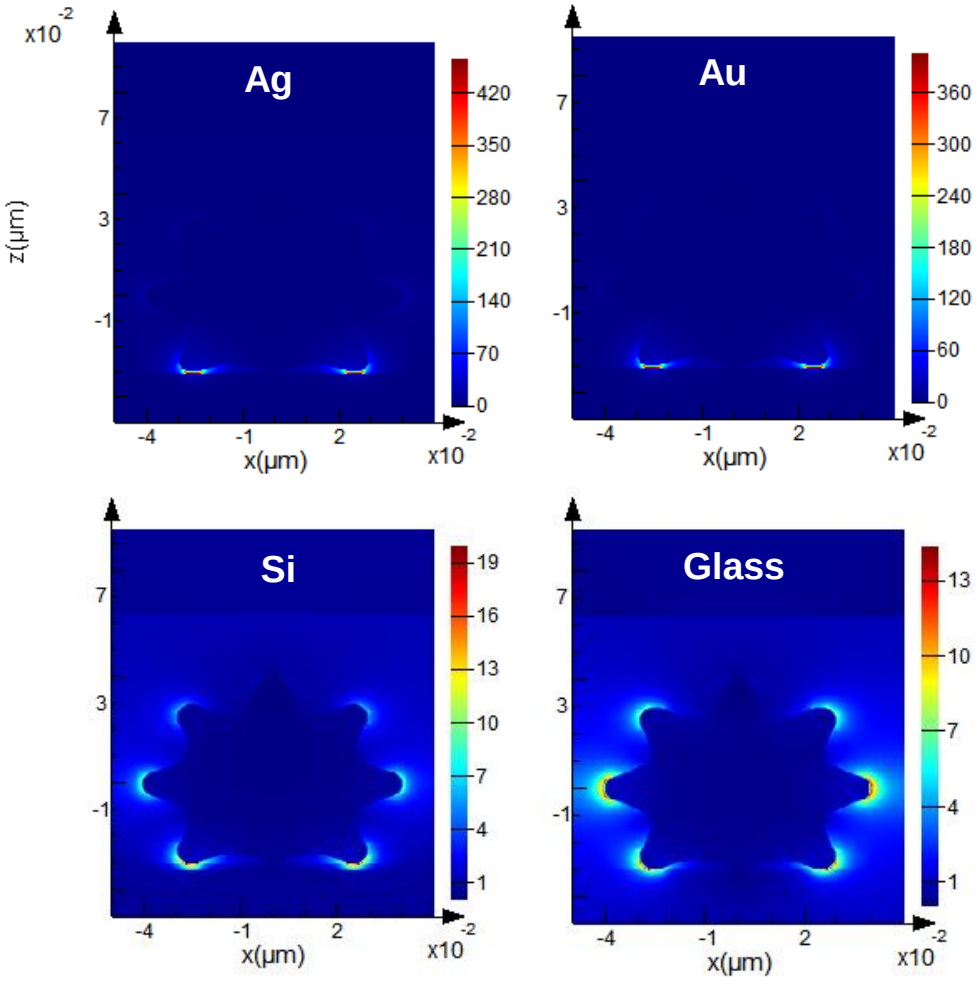

Figure S4. Finite difference time domain (FDTD) simulation of the localized E-fields of the hexagonal GNS assemblies on Ag, Au, Si, and glass substrates with an interparticle separation of 10 nm.

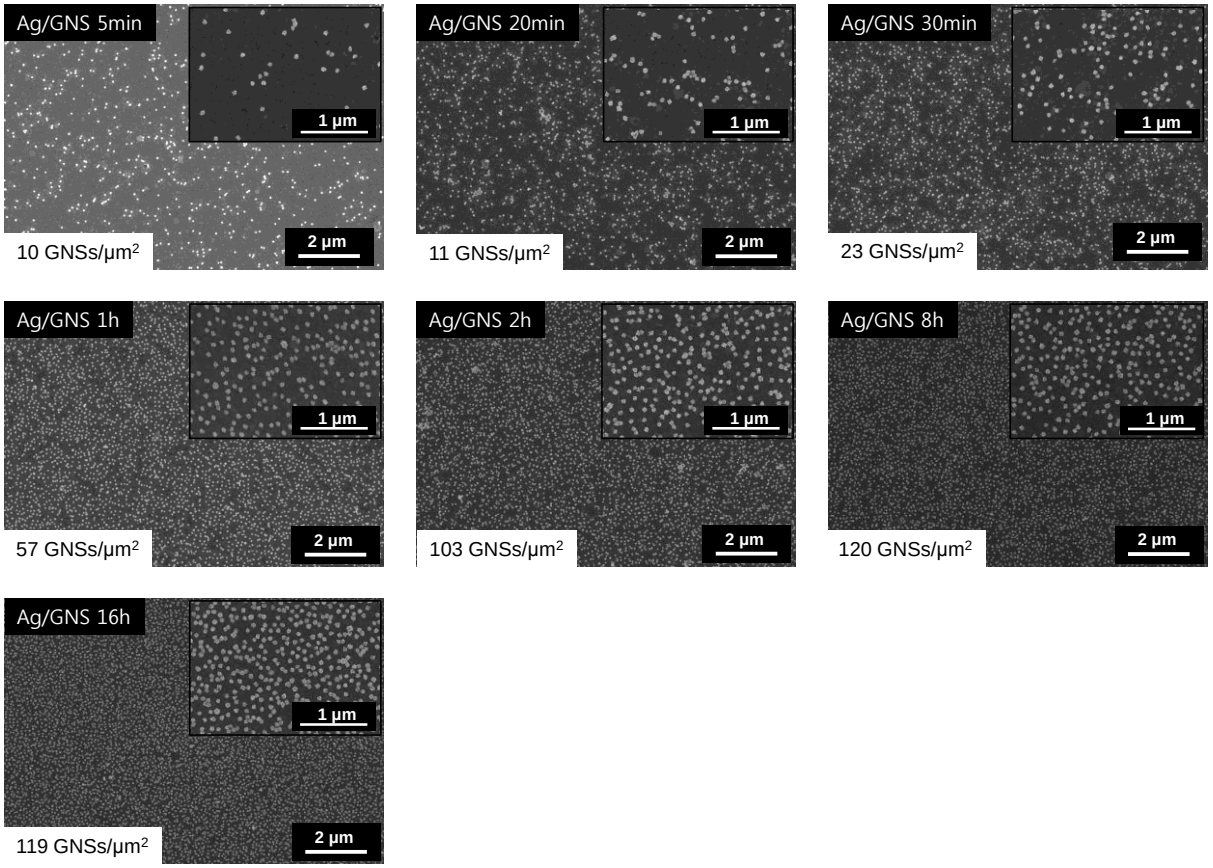

Figure S5. FE-SEM images showed different density of GNS assemblies controlled by varying the dipping time from 5 min to 16 hrs.

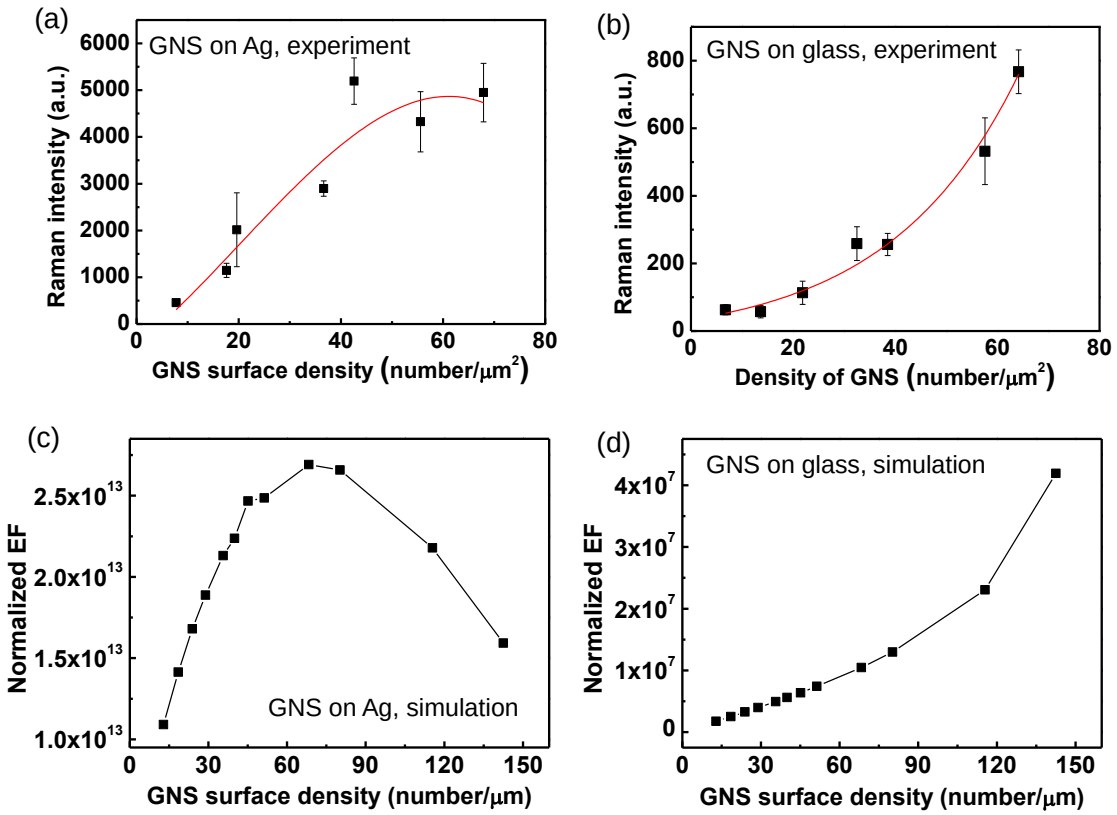

Figure S6. (a) and (b) SERS intensities as a function of gold nanostar surface densities on (a) Ag and (b) glass substrates. (c) and (d) FDTD calculation of normalized SERS enhancement factor (EF) as a function of gold nanostar density on (c) Ag and (d) glass substrates.

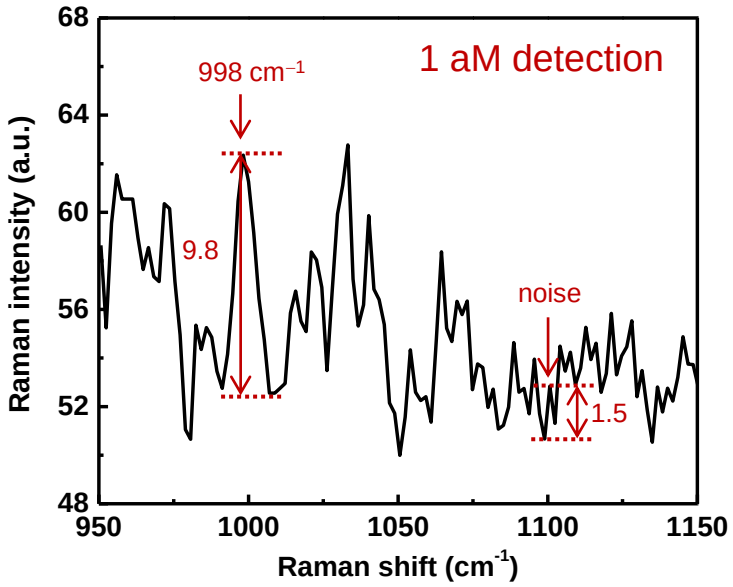

Figure S7. Raman spectrum of 1 aM BT with the signal to noise ratio (S/N) of 6.5.

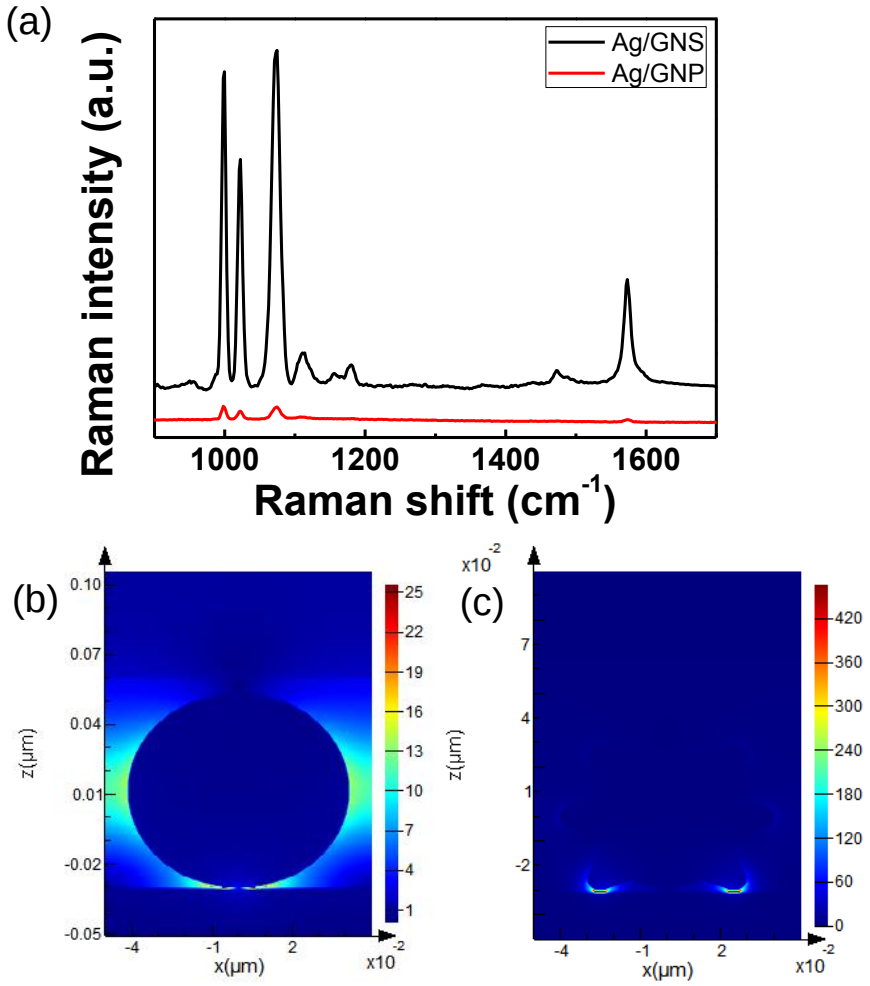

Figure S8. (a) The SERS spectra of benzenethiol (0.1%) adsorbed on the GNSs or nanospheres assembled on Ag films. (b) and (c) FDTD simulated electromagnetic field distributions of (b) spherical gold nanospheres and (c) GNSs on Ag films under excitations of 785nm laser.

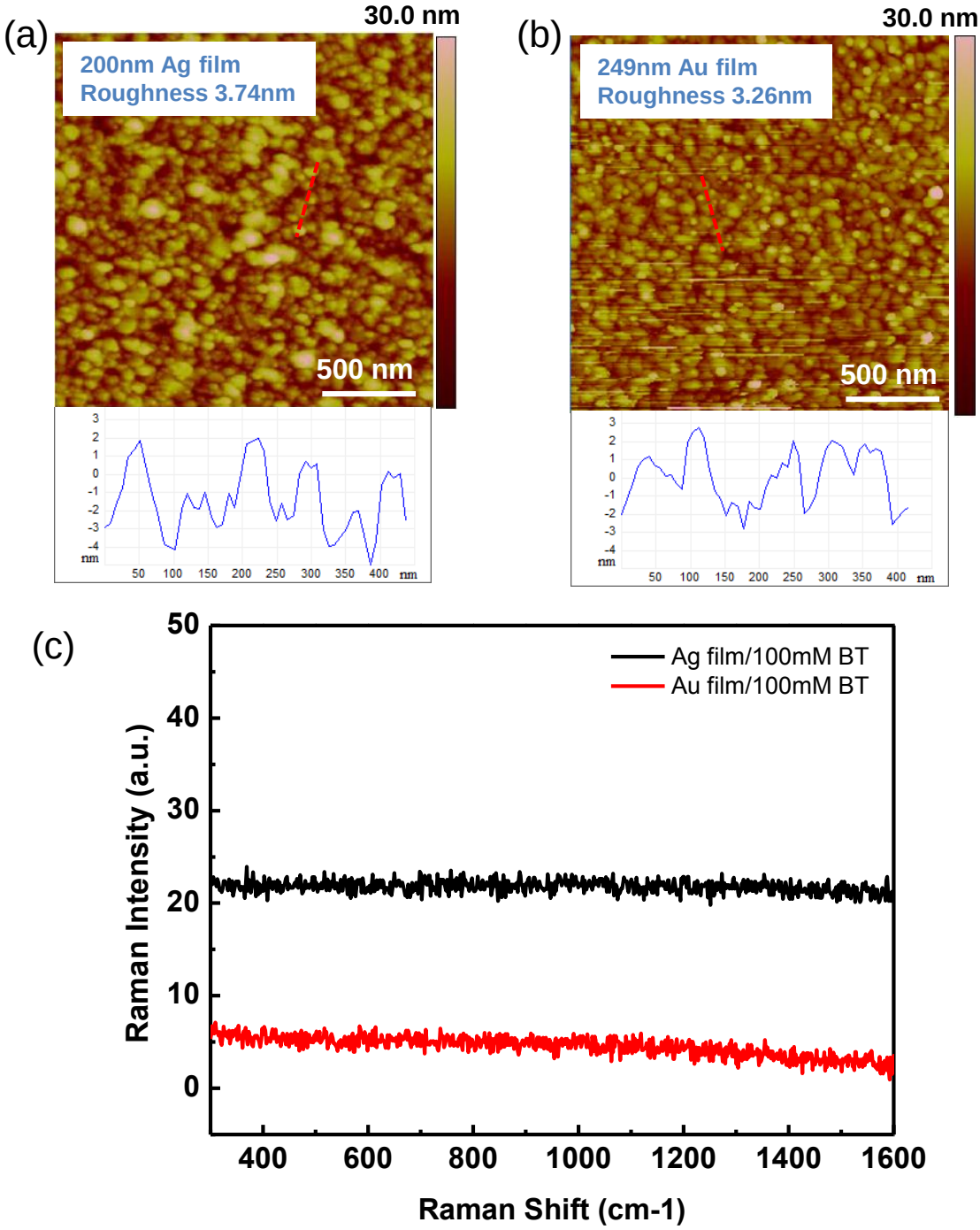

Figure S9. (a) and (b) AFM images and cross section measurement to show the roughness of Ag and Au fims. (c) SERS spectra of 100 mM benzenethiol on Ag and Au films showing no measurable Raman spectra.

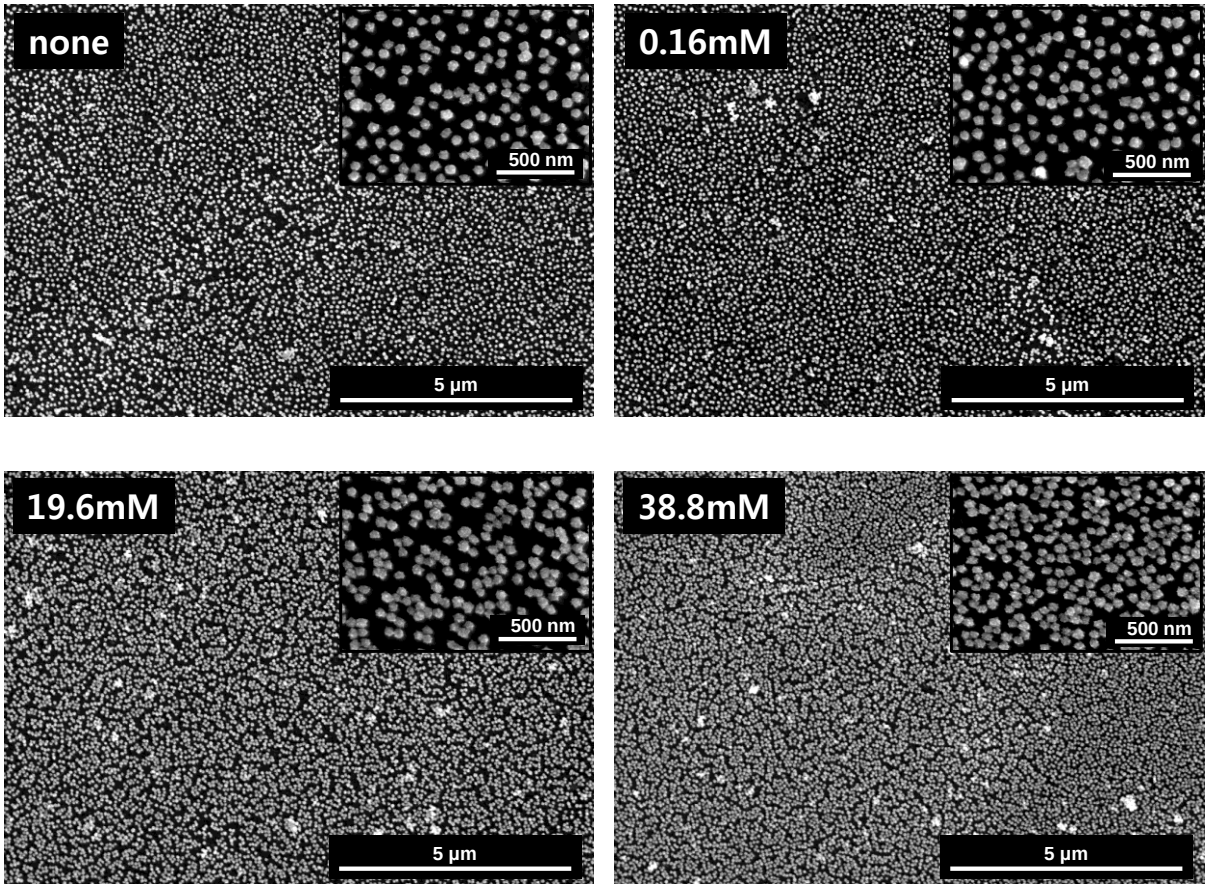

Figure S10. FE-SEM images of GNS assemblies on Ag films prepared by four different sodium citrate solutions: none, 0.16 mM, 19.6 mM, and 38.8 mM, where the increase of sodium citrate concentration resulted in the increase of GNS surface density.

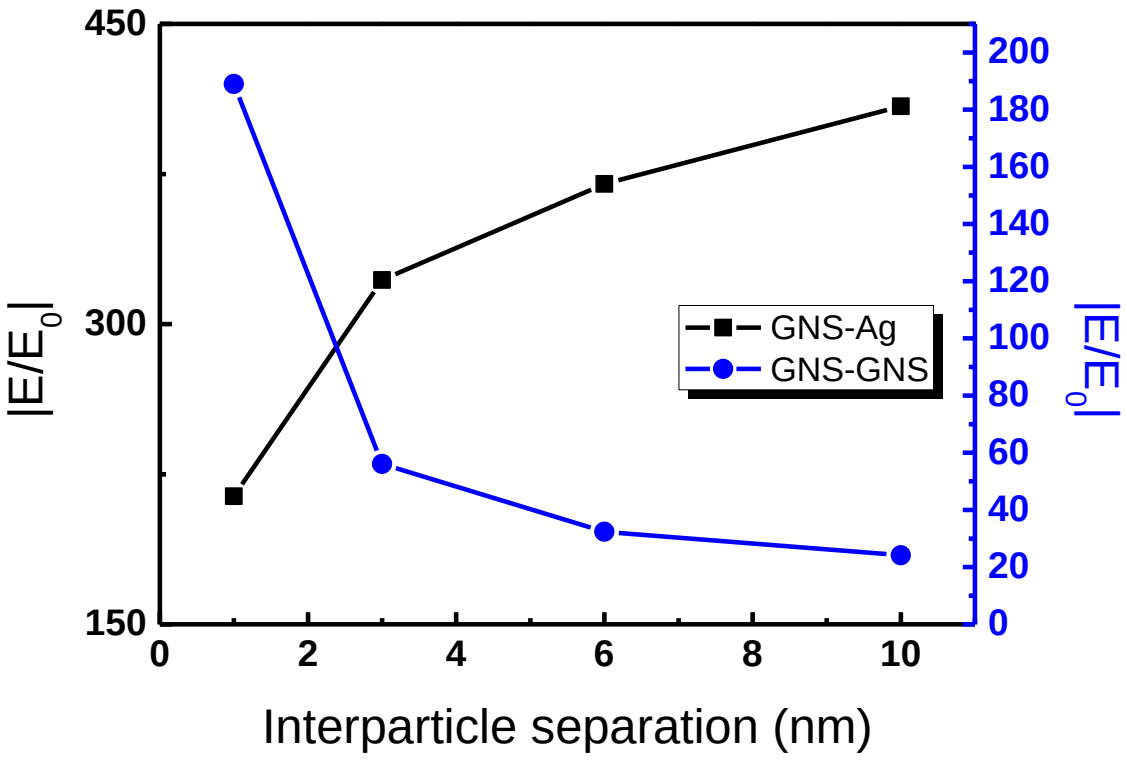

Figure S11. FDTD Simulation of local E-fields at the GNS-Ag gap and GNS-GNS gap.

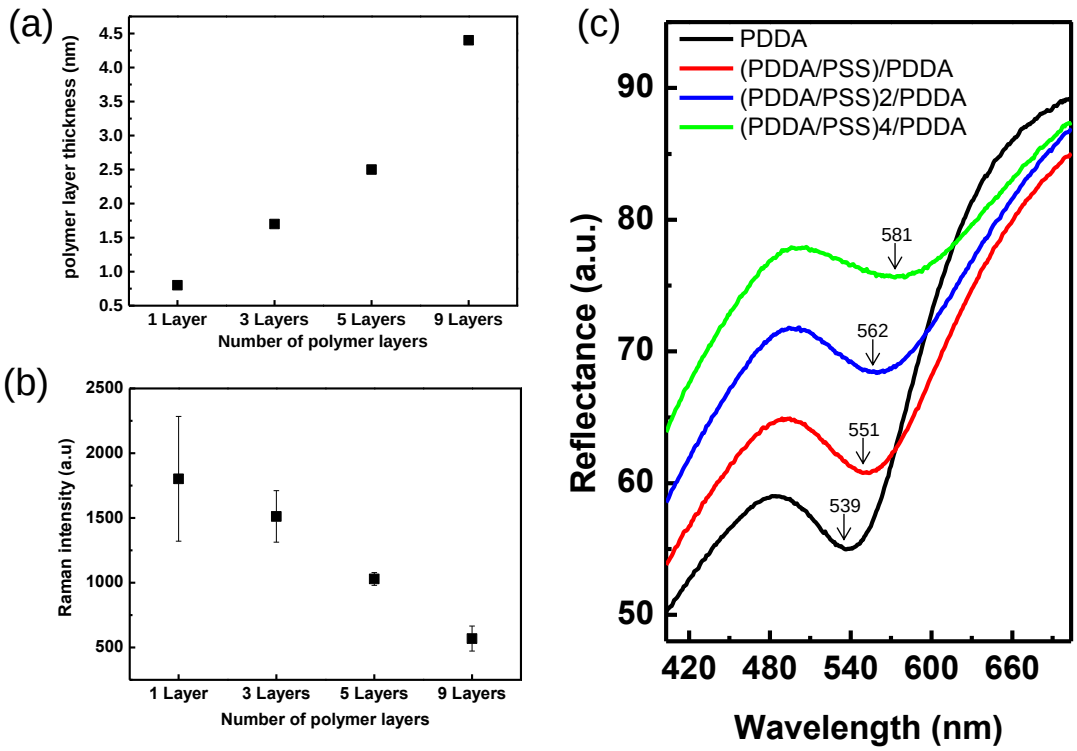

Figure S12. (a) The variation of polymer layer thickness with the change of layer numbers of the polymer layers; 1 layer for PDDA, 3 layers for (PDDA/PSS)PDDA, 5 layers for $(PDDA/PSS)_2PDDA$, and 9 layers for $(PDDA/PSS)_4PDDA$. (b) SERS intensity variation with the change of polymer layer numbers for the detection of 100mM benzenethiol molecules. (c) The reflectance spectra of GNS assemblies (~120 GNSs/μm^2) on Ag substrates with different thickness of polymer layers.

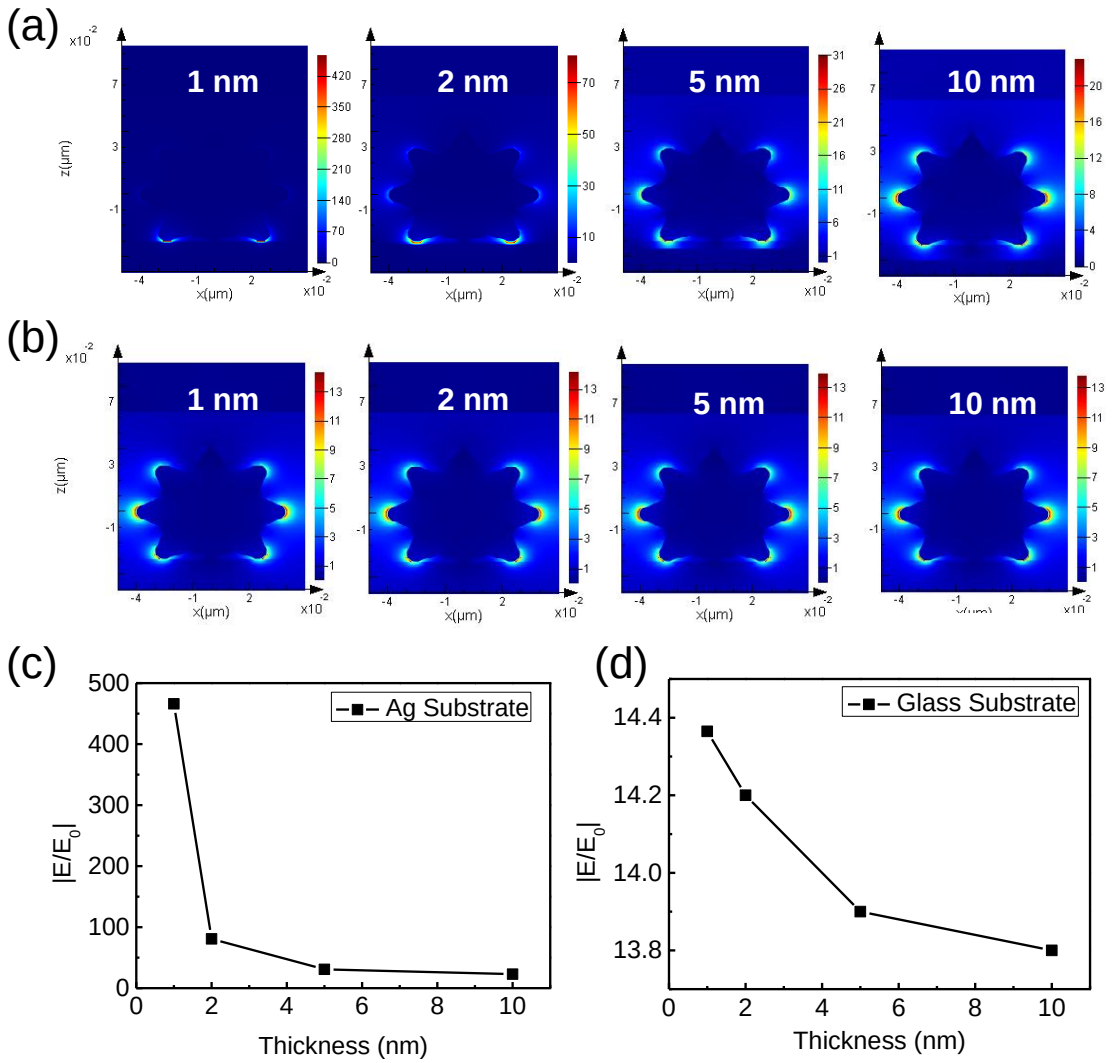

Figure S13. FDTD simulations of E-fields for GNS assemblies on Ag (a) and glass (b) substrates with the change of the gap distances (1 – 10 nm) between the GNS and the substrates. Local E-fields at different gap distances for (c) GNS-Ag film and (d) GNS-glass substrate.

References

1. F. J. GarciaVidal and J. B. Pendry, *Phys. Rev. Lett.*, 1996, **77**, 1163-1166.

2. N. A. Hatab, C.-H. Hsueh, A. L. Gaddis, S. T. Retterer, J.-H. Li, G. Eres, Z. Zhang and B. Gu, *Nano Lett.*, 2010, **10**, 4952-4955.

3. L. Rodriguez-Lorenzo, R. A. Alvarez-Puebla, I. Pastoriza-Santos, S. Mazzucco, O. Stephan, M. Kociak, L. M. Liz-Marzan and F. J. Garcia de Abajo, *J. Am. Chem. Soc.*, 2009, **131**, 4616-4618.

4. J. B. Jackson and N. J. Halas, *Proc. Natl. Acad. Sci. U.S.A.*, 2004, **101**, 17930-17935.

5. C. L. Haynes and R. P. Van Duyne, *J. Phys. Chem. B*, 2003, **107**, 7426-7433.

6. J. M. McLellan, Z.-Y. Li, A. R. Siekkinen and Y. Xia, *Nano Lett.*, 2007, **7**, 1013-1017.

7. H. Schnitzler and K.-P. Zimmer, Advances in stereomicroscopy, 2008.